IMPACT OF DOMINANT WAVES ON SEA DRAG

V. K. MAKIN
Royal Netherlands Meteorological Institute (KNMI), De Bilt, The Netherlands

V. N. KUDRYAVTSEV
Marine Hydrophysical Institute, Sebastopol, Ukraine

(Received in final form 13 September 2001)

Abstract. The impact of air-flow separation from breaking dominant waves is analyzed. This impact results from the correlation of the pressure drop with the forward slope of breaking waves. The pressure drop is parameterized via the square of the reference mean velocity. The slope of breaking waves is related to the statistical properties of the wave breaking fronts described in terms of the average total length of breaking fronts. Assuming that the dominant waves are narrow and that the length of breaking fronts is related to the length of the contour of the breaking zone it is shown that the separation stress supported by dominant waves is proportional to the breaking probability of dominant waves. The breaking probability of dominant waves, in turn, is defined by the dominant wave steepness. With the dominant wave steepness increasing, the breaking probability is increased and so does the separation stress. This mechanism explains wave age (younger waves being steeper) and finite depth (the spectrum is steeper in shallow water) dependence of the sea drag. It is shown that dominant waves support a significant fraction of total stress (sea drag) for young seas due to the air-flow separation that occurs when they break. A good comparison of the model results for the sea drag with several data sets is reported.

Keywords: Air-flow separation, Dominant waves, Sea drag, Wave age, Wind waves.

1. Introduction

In Kudryavtsev and Makin (2001) we developed an approach that accounts for the impact of the air-flow separation (AFS) from breaking waves on the sea drag in the frame of the wind-over-waves coupling theory developed by Makin et al. (1995), Makin and Kudryavtsev (1999), and Kudryavtsev et al. (1999). This impact results from the correlation of the pressure drop with the forward slope of breaking waves. The pressure drop is parameterized via the square of the reference mean velocity. The slope of breaking waves is related to the statistical properties of the wave breaking fronts described in terms of a distribution function $\Lambda(\mathbf{c})$ such that $\Lambda(\mathbf{c})d\mathbf{c}$ represents the average total length per unit surface area of breaking fronts that have velocities in the range $\mathbf{c}$ to $\mathbf{c} + d\mathbf{c}$. Wave breaking statistics were introduced originally by Phillips (1985). He related this quantity to the rate of energy dissipation due to wave breaking. To avoid the poorly-known quantity $\Lambda(\mathbf{c})$ in the description of the air-flow separation we instead used in Kudryavtsev and Makin (2001) the rate of energy dissipation. The advantage of this approach is that the rate of energy

Boundary-Layer Meteorology **103:** 83–99, 2002.

dissipation can be estimated from the energy balance in the equilibrium range of the wind-wave spectrum. The equilibrium range is defined at wavenumbers large compared with that of the spectral peak (Phillips, 1985). We further assumed that the rate of energy dissipation in the equilibrium range is proportional to the energy input from the wind. We have shown that the separation stress contributes significantly to the total stress (sea drag) for a fully developed sea supporting up to about 50% of the stress at high wind speeds. We also showed that the main contribution to the separation stress comes from the shortest waves (wavelength shorter than 1 m) simply due to their high surface density. The role of waves at the spectral peak appeared to be negligible for a fully developed sea; the role of dominant waves (i.e., waves at the spectral peak) for developing seas was not analyzed. However, there is recent experimental evidence (Banner et al., 2000) that dominant waves do break, with the probability of wave breaking events approaching 15% in the open ocean. In small water bodies such as lakes the dominant waves break intensively contributing up to 60% to the probability of wave breaking events (Babanin et al., 2001). It is anticipated that dominant waves could also contribute to the separation stress and thus impact upon the sea drag.

Banner et al. (2000) and Babanin et al. (2001) relate the breaking probability of dominant waves to the dominant wave steepness defined through the significant wave height taken around the spectral peak and the spectral peak wavenumber. The steeper the dominant waves are the higher is their breaking probability. In this paper we suggest that the separation stress supported by breaking dominant waves is proportional to their breaking probability. If that is so, steeper dominant waves support more separation stress increasing their impact on the sea drag. This can immediately explain an experimental fact that young seas have an increased surface roughness as compared to a fully developed sea (e.g., Donelan et al., 1993; Drennan et al., 2002; Maat et al., 1991; Oost et al., 2002; Smith et al., 1992). The 'young' dominant waves are steeper and thus contribute more to the separation stress. This also explains a known experimental fact that the drag coefficient is higher in the shallow waters as compared to the open ocean data (Geernaert, 1990; Oost, 1998; Smith et al., 1992). When waves propagate into the shallow water the long dominant waves begin to feel the bottom and become steeper (Geernaert et al., 1986; Young and Verhagen, 1996). Hence, depth-limited spectra could be expected to be more peaked compared to spectra in deep water (Young and Verhagen, 1996). That leads to enhanced breaking and, therefore, to enhanced separation of the air flow and enhanced sea drag. Recent indirect evidence that dominant waves play an important role in supporting the sea drag comes from Taylor and Yelland (2001). They proposed that the sea roughness can be predicted from the significant wave height and the dominant wave steepness, and have shown that the proposed formula predicts well the magnitude and behaviour of the drag coefficient as observed in wave tanks, lakes, and the open ocean. The set of physical processes needed to explain the newly reported sets of field observations is incomplete. This therefore requires a more complete theory, i.e., with fewer assumptions.

In this paper we extend our 'separation' model (Kudryavtsev and Makin, 2001) to account for the impact of air-flow separation from breaking dominant waves on the sea drag. We basically follow the approach described in Kudryavtsev and Makin (2001) but will distinguish the separation stress supported by waves in the equilibrium range and the stress supported by dominant waves. To parameterize the latter we use the results by Longuet-Higgins (1957) who derived the statistical properties for a random, moving, Gaussian surface. The assumption is that dominant waves can be considered as narrow and close to long-crested waves. Starting from the expression by Longuet-Higgins for the length of contours and relating the height of the contour to the amplitude of breaking wave we relate the length of contours to the average total length per unit surface area of breaking fronts of dominant waves $\Lambda(\mathbf{c})d\mathbf{c}$. The separation stress due to breaking of dominant waves can now be calculated through $\Lambda(\mathbf{c})d\mathbf{c}$ in a general manner as suggested by Kudryavtsev and Makin (2001). The rest of the model by Kudryavtsev and Makin (2001) remains the same, except that now the separation stress is presented as a sum of separation stress from waves in the equilibrium range and separation stress from dominant waves.

Under the assumptions introduced into the model we show that dominant waves could support a significant part of the separation stress. The separation stress due to dominant waves is defined by their steepness. We show that the sea drag increases with the inverse wave-age parameter in good agreement with measurements. It is interesting to note that for the application to very young waves characteristic of laboratory conditions the model predicts a decrease of the drag with an increase of the inverse wave-age parameter in agreement with measurement. This is explained by the fact that the wave spectrum in the laboratory conditions is very narrow in wavenumber range and supports less separation stress than in the open ocean. Besides, the reference wind velocity triggering the separation drops rapidly for shorter waves. The model reproduces as well the increase of the sea drag with decreasing of the water depth. We make an interpretation of the HEXMAX, the HEXOS Main Experiment (where HEXOS refers to Humidity Exchange Over the Sea), as reported by Janssen (1997) and show a good correspondence of model results to data.

2. Drag of the Sea Surface Accounting for the AFS

2.1. The Model

A concise description of the model of Kudryavtsev and Makin (2001) is presented in this section. The model is based on the conservation equation for integral momentum

$$u_*^2 = \tau^\nu + \tau^w + \tau^s, \tag{1}$$

where the friction velocity u_* is taken outside the wave boundary layer, i.e., at a height where the impact of waves vanishes. In (1) τ^ν is the viscous stress at the sea surface, τ^w is the wave-induced flux at the surface, and τ^s is the surface flux supported by the AFS. All stresses are normalized by the density of air ρ_a.

Patching the linear wind profile inside the viscous layer with the logarithmic wind profile above it, the viscous stress can be written

$$\tau^\nu = (\kappa d)^{-1} \frac{\delta}{z_0} u_*^2, \tag{2}$$

where

$$\delta = d \frac{\nu}{u_*} \tag{3}$$

is the thickness of the viscous sublayer, ν is the molecular viscosity, $d = 12$ is a constant, and z_0 is the roughness parameter defined through the logarithmic wind profile extending to the surface from a height where the wind velocity is not influenced by wave motions

$$U(z) = \frac{u_*}{\kappa} \ln \frac{z}{z_0}, \tag{4}$$

where κ is the von Karman constant.

The wave-induced stress is

$$\tau^w = \int_k \int_\theta \beta c^2 B(k, \theta) \cos\theta d \ln k d\theta, \tag{5}$$

where $B(k, \theta)$ is the saturation wave spectrum, β is the growth rate parameter specified in the form

$$\beta = C_\beta \left(\frac{u_*}{c}\right)^2 \cos^2\theta, \tag{6}$$

where k is the wavenumber, c is the phase velocity, and θ is the angle. The proportionality coefficient C_β is

$$C_\beta = a_1 \kappa^{-1} \ln \frac{\pi}{k z_c}, \tag{7}$$

where $z_c = z_0 \exp(\kappa c/(u_* \cos\theta))$ is the height of the critical layer, and the value of a_1 is close to 2. With (6) the relation (5) takes the form

$$\tau^w = u_*^2 \int_k \int_\theta C_\beta B \cos^3\theta d\theta d \ln k. \tag{8}$$

It was shown that the separation stress supported by the AFS from all waves has a general form

$$\tau^s = \varepsilon_b \gamma \int_{\mathbf{c}} u_s^2 \cos\theta k^{-1} \Lambda(\mathbf{c}) d\mathbf{c}, \tag{9}$$

where the reference wind speed u_s

$$u_s = \frac{u_*}{\kappa} \cos\theta \ln \frac{1}{kz_0} - c \tag{10}$$

is specified at the level $z_b = 1/k$, $\varepsilon_b = 0.5$ is the characteristic slope of the breaking wave, and $\gamma = 1$ is an empirical constant. We shall now distinguish the separation stress supported by waves in the equilibrium range of the spectrum and the separation stress supported by dominant waves around the spectral peak, i.e.,

$$\tau^s = \tau^s_{eq} + \tau^s_d. \tag{11}$$

The separation stress supported by waves in the equilibrium range of the spectrum τ^s_{eq} was obtained by Kudryavtsev and Makin (2001). Following the approach by Phillips (1985) we directly related the distribution function $\Lambda(\mathbf{c})$ to the average rate of the energy dissipation per unit area by breakers with velocities between $\mathbf{c}$ and $\mathbf{c}+d\mathbf{c}$. We further assumed that, under steady conditions, the energy dissipation due to wave breaking is equal to or proportional to the energy input from the wind in the equilibrium range of the wind-wave spectrum. We then showed that the total length of wave breaking fronts can be expressed in terms of the saturation spectrum as

$$\Lambda(\mathbf{c}) \sim \frac{\beta}{b} B(\mathbf{c}) k^{-1} \tag{12}$$

with $b = 0.01$ being an empirical constant. The shape of the saturation spectrum was calculated from a theoretical model for the short wave spectrum by Kudryavtsev et al. (1999). With (12) the separation stress (9) can be written as

$$\tau^s_{eq} = C_s u_*^2 \int_\theta \int_{k<k_m} \ln^2(\varepsilon_b / kz_c) \beta(k,\theta) B(k,\theta) \cos^3\theta d\theta d \ln k, \tag{13}$$

where $C_s = \varepsilon_b \gamma / (b\kappa^2)$ is a constant. The integration over wavenumber k in (13) is done in the wavenumber range satisfying the condition $k < k_m$, where $k_m = 2\pi/\lambda_m$ rad m^{-1} and $\lambda_m = 0.1$ m. This condition reflects the fact that waves shorter than λ_m generate parasitic capillaries rather than break, as discussed by Kudryavtsev et al. (1999). The generation of parasitic capillaries prevents the formation of the sharp surface slope and hence prevents the separation of the air flow from these short waves.

Equation (1) with (2), (8), and (13) with the given model for the saturation wave spectrum can be solved by iterations to obtain the roughness parameter of the sea surface and thus the sea drag as a function of the wind speed U_{10} taken at 10-m height.

The separation stress supported by dominant waves for developing seas τ_d^s was not considered in our previous paper Kudryavtsev and Makin (2001). Its description is given below.

2.2. Stress supported by the AFS from dominant waves

It is anticipated that breaking dominant waves contribute to the separation stress and thus impact the sea drag. Let us define the range of dominant waves by the condition $k \leq 2k_p$, where k_p is the spectral peak wavenumber. We have to define now $\Lambda(\mathbf{c})$ for dominant waves. In the range of dominant waves Equation (12) does not hold, because the assumption that the dissipation is balanced by the wind input is not valid in the range of the spectral peak.

The statistics of dominant wave breaking will be described by a breaking model based on a concept of a threshold level. This model is based on the description of the statistical properties of the Gaussian wave surface, where it is assumed that the wave breaking event takes place when the sea surface exceeds some threshold level. This approach was applied for the description of wave breaking statistics by Srokosz (1985) and Xu et al. (2000). Here we use the detailed analysis of statistical properties for a random, moving, Gaussian surface given by Longuet-Higgins (1957). He derived a general expression for the mean length of a contour for the cross-section of the wavy surface by a plane of a constant height $\zeta = \zeta_0 = \text{const}$ per unit area $\overline{s}$ (his Equation 2.3.16). Assuming that dominant waves can be presented as a superposition of narrow band random surface waves this expression takes the form

$$\overline{s} = \frac{1}{\pi}\left(\frac{m_{20}}{m_{00}}\right)^{1/2} \exp\left(-\frac{\zeta_0^2}{2m_{00}}\right), \tag{14}$$

where the spectral moments of order mn: $m_{mn} = \int k_1^m k_2^n S(\mathbf{k}) d\mathbf{k}$ and $S = k^{-4}B$. For the narrow spectrum the ratio m_{20}/m_{00} defines the mean wavenumber k_m^2. The mean wavenumber k_m is very close to the spectral peak wavenumber k_p.

For dominant waves defined above in the range $k < 2k_p$ we can write for the surface variance of the dominant waves

$$m_{00} = \int_0^{2k_p} B(k, \theta) k^{-2} d \ln k d\theta. \tag{15}$$

The second-order moment of the dominant waves is $m_{20} = \int_0^{2k_p} B(k, \theta) k^{-1} d \ln k d\theta$. Let us define ζ_0 as the height of a contour above which the onset of dominant wave breaking occurs. Here, we assume that when the surface level ζ exceeds the 'threshold' level ζ_0, a strong and sudden (explosive) instability erupts and causes the onset of breaking. Multiplying the nominator and denominator of a ratio under the exponential in relation (14) by $2k_m^2$ we obtain

$$\overline{s} = \frac{1}{\pi} k \exp\left(-\frac{\varepsilon_T^2}{\varepsilon_s^2}\right), \tag{16}$$

where $\varepsilon_s = 2k_m m_{00}^{1/2}$ is the dominant wave steepness and $\varepsilon_T = \sqrt{2}\zeta_0 k_m$ is a tuning constant. The wave breaking model based on a concept of the threshold level (Equation (16)) gives the length of the contours of the breaking zone. Taking into account that the length of breaking fronts is approximately twice less than $\overline{s}$, the average total length per unit surface area of breaking fronts of dominant waves is

$$\Lambda(\mathbf{c})d\mathbf{c} = \frac{1}{2\pi} k \exp\left(-\frac{\varepsilon_T^2}{\varepsilon_s^2}\right). \tag{17}$$

The exponential in (17) describes the breaking probability of dominant waves as defined by Srokosz (1985)

$$b_T = \exp\left(-\frac{\varepsilon_T^2}{\varepsilon_s^2}\right). \tag{18}$$

With (17) and (19) the separation stress (9) supported by dominant waves is

$$\tau_d^s = \frac{\varepsilon_b \gamma}{2\pi} u_{sd}^2 b_T. \tag{19}$$

Here the reference wind speed for dominant waves u_{sd}

$$u_{sd} = \frac{u_*}{\kappa} \ln \frac{\varepsilon_b}{k_m z_0} - c_m \tag{20}$$

is specified at the level just above the breaking dominant waves, i.e., at $z_b = \varepsilon_b / k_m$, and c_m is the mean phase speed of dominant waves.

3. Results

3.1. Specification of the Wave Spectrum

To obtain the roughness parameter as a function of wind speed and wave age an empirical wave spectrum or a physical model of the wave spectrum can be used. To calculate the stress due to the AFS supported by short gravity waves τ_{eq}^s, the equilibrium part of the wave spectrum defined at $k < k_m$ has to be known. The calculation of the separation stress supported by dominant waves τ_d^s requires the shape of the spectrum at the spectral peak, while the calculation of the wave-induced stress τ^w requires the shape of the spectrum in the wavenumber range from capillary waves to the spectral peak. As in Kudryavtsev and Makin (2001) we use here a model of the wave spectrum suggested by Kudryavtsev et al. (1999), which describes the saturation spectrum $B(k, \theta)$ in the full wavenumber range from a few millimetres up to the spectral peak. It consists of two parts: the low and the high wavenumber spectrum

$$B(k, \theta) = B_l(k, \theta) + B_h(k, \theta). \tag{21}$$

The shape of the low wavenumber spectrum B_l is given by the empirical model of Donelan et al. (1985) with the correction proposed by Elfouhaily et al. (1997). The spectral shape of B_l is defined by the inverse wave-age parameter U_{10}/c_p (c_p is the phase speed at the spectral peak). The shape of the high wavenumber spectrum B_h results from the physical model developed by Kudryavtsev et al. (1999). The model is based on the energy balance equation and accounts for wind input, viscous dissipation, dissipation due to wave breaking (including energy losses due to generation of parasitic capillaries by short gravity waves), and non-linear three-wave interaction. The details of the model can be found in Kudryavtsev et al. (1999).

For a given wind speed the model provides the sea-surface roughness parameter z_0, which is a function of the saturation spectrum B. The saturation equilibrium spectrum B_h in turn depends on the momentum flux, which is defined by the sea surface roughness z_0. Thus the wind waves and the atmospheric boundary layer are strongly coupled forming a self-consistent dynamical system.

3.2. Modelled Probability of Wave Breaking

Recent analysis of the breaking statistics of the dominant waves by Banner et al. (2000) has shown that dominant waves contribute significantly to the breaking probability of waves b_T. Their analysis of data obtained during several campaigns shows that b_T can reach about 15% in the open ocean. They argue that the nonlinear hydrodynamic processes associated with wave groups are responsible for the onset of dominant wave breaking. They further related the breaking probability of dominant waves to the significant spectral peak steepness defined by $\epsilon_s = H_d k_p/2$, where the significant wave height for dominant waves H_d is very close to $4m_{00}^{1/2}$, so that $\epsilon_s \simeq \varepsilon_s$ as defined earlier. They further show a strong dependence of the breaking probability on the steepness.

The modelled probability of dominant wave breaking b_T as a function of the inverse wave age U_{10}/c_p is shown in Figure 1, together with data from the Black Sea data set reported by Banner et al. (2000), their Table 1. This data set was chosen as it covers a wide range of the wave-age parameter, which is closely related to the dominant wave steepness. A value of 0.1% was assigned to the reported zero value

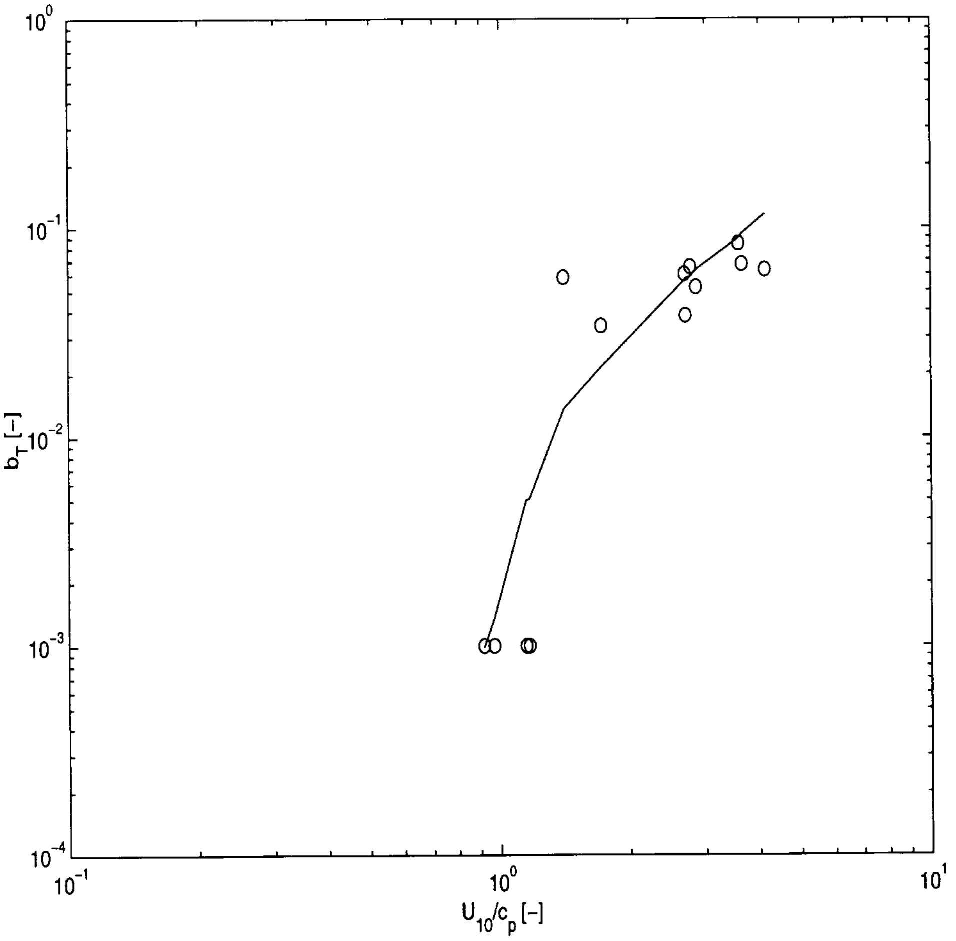

Figure 1. Probability of dominant waves breaking b_T versus inverse wave age U_{10}/c_p. Circles, the Black Sea data set reported by Banner et al. (2000); curve, model results.

breaking probability in order to show the points in the figure. The model was evaluated with the wind speed U_{10} and the wave-age parameter specified in the table. The comparison between the model results and data is encouraging considering the fact that the dominant wave-breaking parameter is a difficult quantity to measure. The comparison was obtained with the threshold level for dominant wave steepness $\varepsilon_T = 0.24$. This value is used further throughout the model calculations.

3.3. Role of air-flow separation in forming sea drag

To show the role of the air-flow separation in forming the sea drag the contribution to the total stress u_*^2 of the stress due to the AFS from the equilibrium range τ_{eq}^s/u_*^2, of the stress due to the AFS from the dominant waves τ_d^s/u_*^2, their sum τ^s/u_*^2, and the wave-induced stress τ^w/u_*^2 as a function of the wind speed is shown in Figure 2 for different wave ages. The residual from 1 is the viscous stress (not shown) due to the condition $\tau^v/u_*^2 + \tau^w/u_*^2 + \tau^s/u_*^2 = 1$. For a fully developed sea specified by the inverse wave-age parameter $U_{10}/c_p = 0.83$ dominant waves do not contribute to the stress. Though their breaking occurs (Banner et al., 2000) they propagate with the phase speed exceeding the mean wind speed; the separation cannot occur under such conditions. All the separation stress due to AFS comes from waves in the equilibrium range. For younger seas characterized by increased inverse wave-age parameter, the role of dominant waves in forming the sea drag becomes more and more important. Supporting about 10% of the total stress at $U_{10}/c_p = 2$, and about 20% at $U_{10}/c_p = 3$, their contribution becomes dominant for very young seas $U_{10}/c_p = 5$. The contribution to the sea drag of the stress due to the separation from short waves (equilibrium range) decreases with an increase of U_{10}/c_p. This decrease is explained by the fact that the equilibrium range becomes narrower in wavenumber space with increased inverse wave-age parameter. The separation stress from all waves support 50–60% of the total stress at high wind speeds.

3.4. Wave age and wind speed dependence of the sea drag

The dimensionless roughness length or the Charnock parameter $z_* = z_0 g/u_*^2$ is shown as a function of the inverse wave-age parameter based on the friction velocity u_*/c_p in Figure 3. Calculations are done for the wind speed $U_{10} = 7.5$ m s^{-1} and $U_{10} = 20$ m s^{-1} and the inverse wave-age parameter $0.83 < U_{10}/c_p < 25$. Shallow water effects are not accounted for at this stage. Data are compiled from Donelan et al. (1993), their Figure 2. Model results (as well as data) show a clear increase of the Charnock parameter with increasing inverse wave age. This increase is explained in the present model by the increased steepness of younger waves and thus increased separation stress due to the AFS from dominant waves. Such behaviour of the Charnock parameter could not be explained by the previous version of the model (Kudryavtsev and Makin, 2001) applied to the developing seas, as that model accounts for the separation stress supported by short waves only. The Charnock parameter has a maximum around $u_*/c_p = 0.3 - 0.4$ ($U_{10}/c_p = 7$). For higher values of the inverse wave-age parameter corresponding to very young waves typical for small water bodies and laboratory conditions, the Charnock parameter decreases. This is explained by the fact that the wind-wave spectrum is very narrow in wavenumber space, and the separation stress from the equilibrium range becomes smaller. The dominant waves are very peaked but small in height, and the reference speed (20) is rapidly dropping reducing the separation stress from dominant waves. Both effects lead to decreasing of the Charnock parameter. Despite the large scatter of the data, the model results in general agree well with measurements. It is worthwhile to mention that both HEXMAX and Lake Ontario data were influenced by the shallow water effects not taken into account here. As it becomes clear from the next two sections the shallow water effects lead to

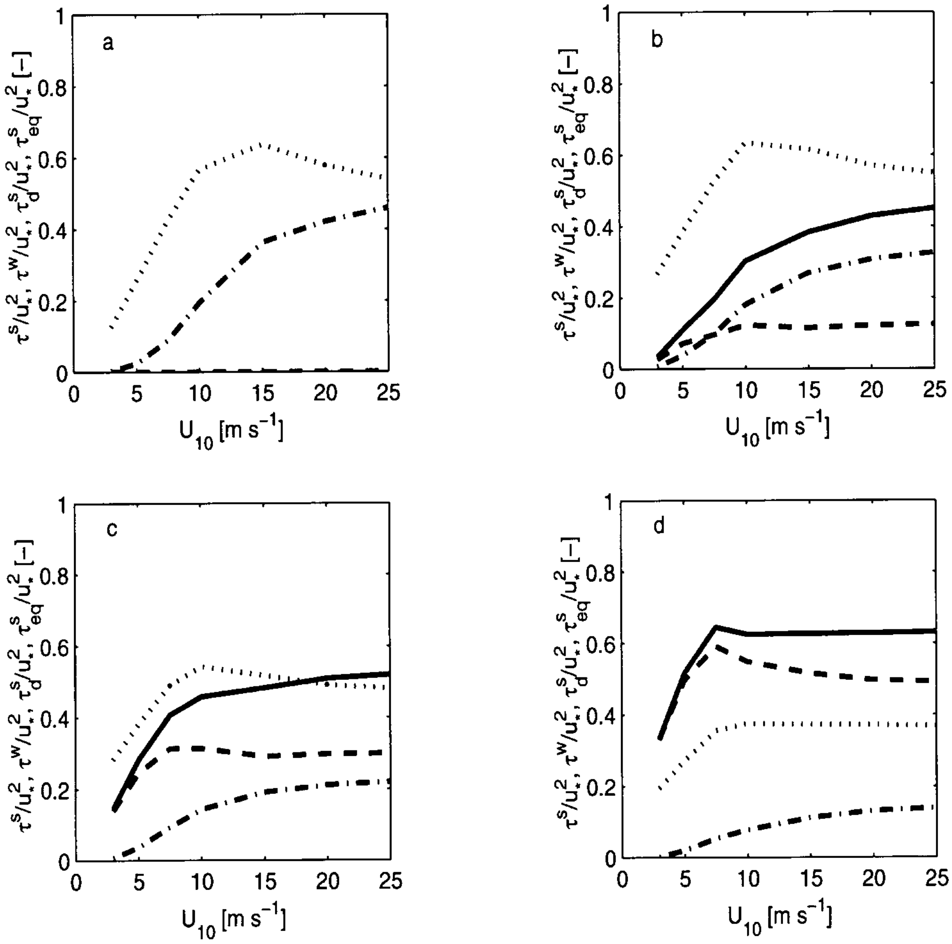

Figure 2. Stress partitioning versus wind speed U_{10}. (a) Inverse wave age $U_{10}/c_p = 0.83$; (b) $U_{10}/c_p = 2$; (c) $U_{10}/c_p = 3$; (d) $U_{10}/c_p = 5$. Dashed line, separation stress due to dominant waves τ_d^s/u_*^2; dashed-dotted line, separation stress due to short waves τ_{eq}^s/u_*^2; solid line, their sum $\tau^s/u_*^2 = \tau_d^s/u_*^2 + \tau_{eq}^s/u_*^2$; dotted line, wave-induced stress τ^w/u_*^2.

enhancement of the sea drag, which can partly explain underestimation of model results for these data sets.

To outline the role of separation from dominant waves we switched off this stress in the model and plot results in the same figure. There is only a marginal increase of the Charnock parameter with increasing inverse wave age. This suggests that the separation from dominant waves is responsible for the observed behaviour of the Charnock parameter with inverse wave age. It is also clear that for waves close to fully developed $u_*/c_p < 0.1$ ($U_{10}/c_p < 1.5$) the dominant waves do not support the separation stress as already explained in the previous section. The

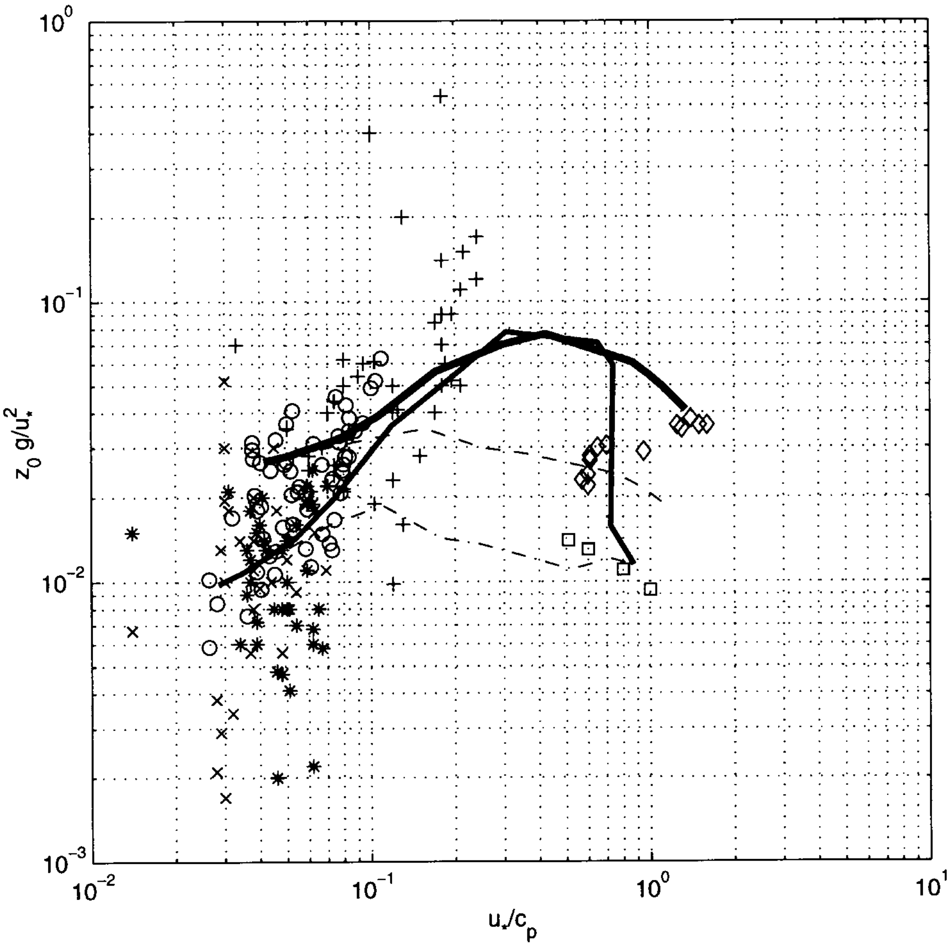

Figure 3. Charnock parameter $z_0 g/u_*^2$ versus inverse wave age u_*/c_p. Model results: Thin solid line, U_{10} = 7.5 m s^{-1}; thick solid line, U_{10} = 20 m s^{-1}, dashed-dotted line, U_{10} = 7.5 m s^{-1} for $\tau_d^s = 0$; dashed line, U_{10} = 20 m s^{-1} for $\tau_d^s = 0$. Symbols indicate data: circles, HEXMAX (Janssen, 1997); pluses, Lake Ontario; stars, Atlantic Ocean, long fetch; x-marks, Atlantic Ocean, Donelan et al. (1993), limited fetch; diamonds, wave tank, Donelan (1990); squares, wave tank, Keller et al. (1992).

Charnock parameter increases with increasing wind speed, the behaviour observed in the open ocean (Yelland and Taylor, 1996).

3.5. Depth dependence of the sea drag

The fact that the AFS from dominant waves contribute a noticeable part to the total stress (sea drag) suggests a mechanism that could explain a known experimental fact that the drag coefficient $C_D = (u_*/U_{10})^2$ is higher in the shallow waters as compared to the open ocean data (Geernaert, 1990; Oost, 1998; Smith et al., 1992).

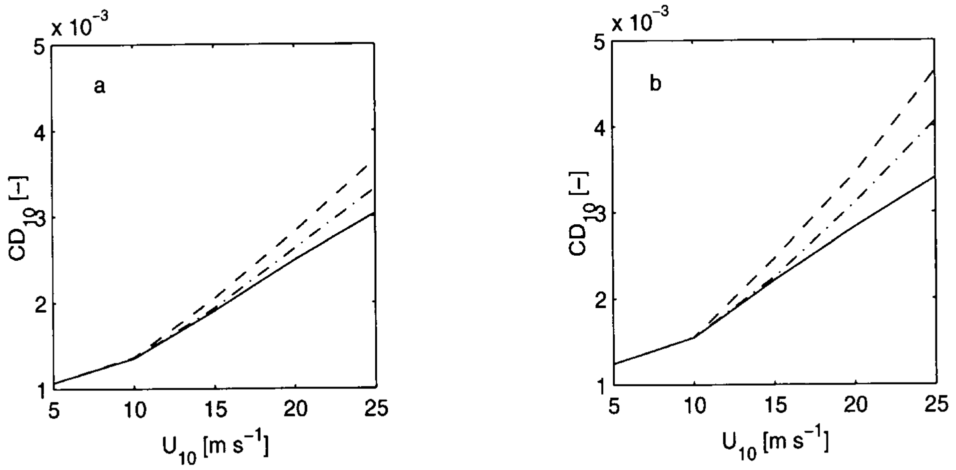

Figure 4. Drag coefficient CD_{10} versus wind speed U_{10} for finite bottom depth. (a) Inverse wave age $U_{10}/c_p = 0.83$; (b) $U_{10}/c_p = 2$. Solid line, infinite depth; dashed-dotted line, 20 m depth; dashed line, 10 m depth.

When waves propagate into the shallow water the long waves begin to feel the bottom and become steeper (Geernaert et al., 1986; Young and Verhagen, 1996). Hence, the depth limited spectra could be expected to be more peaked compared to spectra in the deep water (Young and Verhagen, 1996); this leads to the enhanced breaking of dominant waves. This enhanced breaking leads to the enhanced separation of the air flow from dominant waves, which gives rise to the total stress. To account for this process in our model we need to account for increased peakness of the peak of the wave spectra. We follow a rather crude approach correcting the shape of the low wavenumber spectrum B_l by the peakness parameter γ, which is allowed to depend on the water depth. For that we use the experimental finding of Young and Verhagen (1996) and write

$$\gamma = \gamma_0 - 5.8 \log_{10} \delta, \quad 0.05 < \delta < 1,$$

where γ_0 is the peakness parameter for the spectrum in the deep water, $\delta = gd/U_{10}^2$ is dimensionless depth, and d is depth in metres. Model results for the inverse wave-age parameter $U_{10}/c_p = 0.83$ and 2 are shown in Figure 4. The curves are given for infinite depth, and for 10- and 20-m depth. For a fully developed sea the increase in steepness of dominant waves lead to about 10% increase of the drag coefficient at the wind speed $U_{10} = 20$ m s^{-1}, while for developing waves this increase is about 30%. It is interesting to notice that in the former case the increase is due to the increase of the wave-induced flux. Though the waves become steeper they do not contribute to the separation stress because the reference wind speed is too small to trigger the separation. In the latter case the increase in the drag coefficient is mainly due to the increased separation from peaked dominant waves.

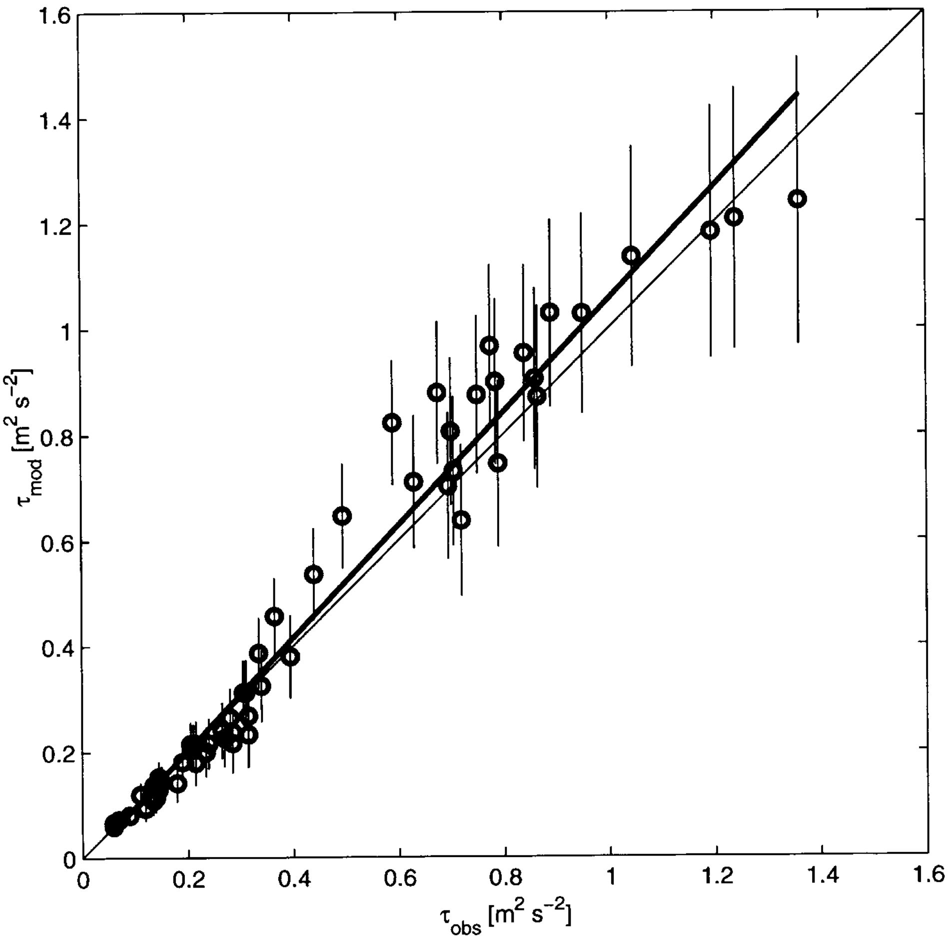

Figure 5. HEXMAX measured stress $\tau_{obs} = u_*^2$ against modelled stress τ_{mod} in m^2 s^{-2}. Bars correspond to the overall error of 20% in measured stress. Thick solid line indicates the regression line.

3.6. Interpretation of HEXMAX data

Finally, we shall make an interpretation of the HEXMAX data set as reported by Janssen (1997). We recall that the site of measurements was situated in 18-m water depth (details see, for example, in Janssen, 1997), and we used this depth in the model. Additional inputs to the model are the wind speed and the phase velocity in the peak of the spectra as listed in the table by Janssen (1997). The seas were approaching a fully developed stage and the inverse wave-age parameter U_{10}/c_p did not exceed 1.9. The wind speed and the stress were measured by pressure and sonic anemometers; we took their average. The scatter plot between measured and modelled stress is shown in Figure 5, with the error bars corresponding to 20% error in stress measurements (Donelan, 1990; Janssen, 1997). The comparison is good; the slope of the regression line is 1.07, while the intercept is -0.014. If we repeat the runs for the same conditions but on the deep water the comparison for the highest four stress points becomes worse as the model will underestimate the stress. A good comparison with data is achieved when both effects, the water depth and the wave-age dependence, are taken into account by the model. If the finite water depth is neglected by the model, it gives underestimation of the stress to about 11% for the last four points on the right side of the plot (as compared to model results shown in Figure 5). If the wave-age dependence is neglected, the underestimation of the stress for the same points reaches about 20%. It is noted here that as the dominant waves play an important role in forming the sea drag by supporting the separation stress the accurate description of this range of the wind wave spectrum is required. We use for the long wave spectrum B_l the empirical spectrum suggested by Donelan et al. (1985). This spectral form represents an averaged wave spectrum obtained from several sets of wave measurements. The form of the empirical spectrum is defined by the wave-age parameter. In reality there is a variability in the spectral form, which can differ for different realizations characterized by the same wave age. In general there is no one-to-one correspondence of the modelled and observed significant wave height and thus the dominant wave steepness. This can partly explain the scatter observed in Figure 5 and in Figure 3, and suggests that for a more accurate comparison of the model results with data the measured spectra specified to the model are required.

4. Summary

The impact of dominant waves – waves at the spectral peak of the wind-wave spectrum – on the sea drag is explained by the air-flow separation, which occurs when the dominant wave breaks. For the description of the stress supported by separation from dominant waves the general approach for the air-flow separation stress developed by Kudryavtsev and Makin (2001) is followed. The separation stress forming a part of the form drag at the sea surface is related to the pressure drop, parameterized via the square of the reference mean velocity, and to the forward slope of breaking waves described in terms of $\Lambda(\mathbf{c})d\mathbf{c}$ – the average total length per unit surface area of breaking fronts that have velocities in the range $\mathbf{c}$ to $\mathbf{c}+d\mathbf{c}$. Starting from the general formula by Longuet-Higgins (1957) for the length of contours, and relating the height of the contour to the amplitude of breaking waves, we relate the length of contours to the average total length per unit surface area of breaking fronts of dominant waves $\Lambda(\mathbf{c})d\mathbf{c}$. To that end the dominant waves are assumed to be narrow and close to long-crested waves. It is further shown that the separation stress supported by dominant waves is proportional to the breaking probability of dominant waves and the reference mean velocity specified at the level just above the breaking dominant wave. The breaking probability of dominant waves in turn is defined by the dominant wave steepness. This is the dominant wave-breaking model based on the concept of the threshold level. With the dominant wave steepness increasing, the breaking probability of dominant waves is increased and so does the separation stress. This mechanism explains why the steep young waves exert more stress than waves in a fully developed sea. The same mechanism explains the finite bottom dependence of the sea drag: long waves propagating into the shallow waters begin to feel the bottom and become steeper. They start breaking more often enhancing the air-flow separation and thus the sea drag. The dependence of the separation stress on the reference velocity, which is a difference of the mean velocity taken just above the breaking wave and its phase velocity, provides a quenching mechanism for fast long waves and very short slow moving waves. The fast waves propagating at the phase speed close to the mean wind speed break but do not induce the air-flow separation because the reference wind speed is too small to trigger the separation. This will explain why long waves propagating into the shallow water at the phase speed exceeding the wind speed support only a marginal fraction of the stress. For the short waves the reference velocity drops because their reference level is too low. That explains the drop in the stress for very young waves typical for the laboratory conditions.

Comparing model predictions to both laboratory and field measurements, we have found good agreement. In this regard, we have demonstrated that for young seas dominant waves support a significant fraction of the total stress (sea drag) due to the air-flow separation that occurs when they break. The separation stress due to dominant waves explains the wave age and finite bottom depth dependence of the sea drag. The exact knowledge of the form of the wind-wave spectrum at the spectral peak becomes of crucial importance in modelling the sea drag for developing seas and shallow waters. That can be provided by direct measurements or by wave prediction models supplied with a correct model for the high frequence tail to account correctly for the stress supported by short waves.

References

Babanin, A. V., Young, I. R., and Banner, M. L.: 2001, 'Breaking Probability for Dominant Waves on Water of Finite Constant Depth', *J. Geophys. Res.* **106**, 11659–11676.

Banner, M. L., Babanin, A. V., and Young, I. R.: 2000, 'Breaking Probability for Dominant Waves on the Sea Surface', *J. Phys. Oceanog.* **30**, 3145–3160.

Donelan, M. A.: 1990, 'Air-Sea Interaction', in *The Sea: Ocean Engineering Science*, Vol. 9, pp. 239–292.

Donelan, M. A., Dobson, F. W., Smith, S. D., and Anderson, R. J.: 1993, 'On the Dependence of Sea Surface Roughness on Wave Development', *J. Phys. Oceanog.* **23**, 2143–2149.

Donelan, M. A., Hamilton, J., and Hui, W. H.: 1985, 'Directional Spectra of Wind Generated Waves', *Phil. Trans. Roy. Soc. London, Ser. A* **315**, 509–562.

Drennan, W. M., Graber, H. C., Hauser, D., and Quentin, C.: 2002, 'On the Wave Age Dependence of Wind Stress over Pure Wind Seas', *J. Geophys. Res.*, in press.

Elfouhaily, T., Chapron, B., Katsaros, K., and Vandemark, D.: 1997, 'A Unified Directional Spectrum for Long and Short Wind Driven Waves', *J. Geophys. Res.* **102**, 15,781–15,796.

Geernaert, G. L.: 1990, 'Bulk Parameterizations for the Wind Stress and Heat Fluxes', in G. L. Geernaert and W. J. Plant (eds.), *Surface Waves and Fluxes*, Vol. 1, Kluwer Academic Publishers, Dordrecht, pp. 91–172.

Geernaert, G. L., Katsaros, K. B., and Richter, K.: 1986, 'Variation of the Drag Coefficient and its Dependence on Sea State', *J. Geophys. Res.* **91**, 1580–1584.

Janssen, J. A. M.: 1997, 'Does Wind Stress Depend on Sea-State or Not? – A Statistical Error Analysis of HEXMAX Data', *Boundary-Layer Meteorol.* **83**, 479–503.

Keller, M. R., Keller, W. C., and Plant, W. J.: 1992, 'A Wave Tank Study of the Determination of X-Band Cross Sections on Wind Speed and Water Temperature', *J. Geophys. Res.* **97**, 5771–5792.

Kudryavtsev, V. N. and Makin, V. K.: 2001, 'The Impact of Air-Flow Separation on the Drag of the Sea Surface', *Boundary-Layer Meteorol.* **98**, 155–171.

Kudryavtsev, V. N., Makin, V. K., and Chapron, B.: 1999, 'Coupled Sea Surface-Atmosphere Model 2. Spectrum of Short Wind Waves', *J. Geophys. Res.* **104**, 7625–7639.

Longuet-Higgins, M. S.: 1957, 'The Statistical Analysis of a Random Moving Surface', *Phil. Trans. Roy. Soc. London, Ser. A* **249**, 321–387.

Maat, N., Kraan, C., and Oost, W. A.: 1991, 'The Roughness of the Sea Surface', *Boundary-Layer Meteorol.* **54**, 89–103.

Makin, V. K. and Kudryavtsev, V. N.: 1999, 'Coupled Sea Surface-Atmosphere Model 1. Wind over Waves Coupling', *J. Geophys. Res.* **104**, 7613–7623.

Makin, V. K., Kudryavtsev, V. N., and Mastenbroek, C: 1995, 'Drag of the Sea Surface', *Boundary-Layer Meteorol.* **79**, 159–182.

Oost, W. A.: 1998, 'The KNMI HEXMAX Stress Data – A Reanalysis', *Boundary-Layer Meteorol.* **86**, 447–468.

Oost, W. A., Komen, G. J., Jacobs, C. M. J., and van Oort, C.: 2002, 'New Evidence for a Relation between Wind Stress and Wave Age from Measurements during ASGAMAGE', *Boundary-Layer Meteorol.*, in press.

Phillips, O. M.: 1985, 'Spectral and Statistical Properties of the Equilibrium Range in Wind Generated Gravity Waves', *J. Fluid Mech.* **156**, 505–531.

Smith, S. D., Anderson, R. J., Oost, W. A., Kraan, C., Maat, N., DeCosmo, J., Katsaros, K. B., Davidson, K. L., Bumke, K., Hasse, L., and Chadwick, H. M.: 1992, 'Sea Surface Wind Stress and Drag Coefficients: The HEXOS Results', *Boundary-Layer Meteorol.* **60**, 109–142.

Srokosz, M. A.: 1985, 'On the Probability of Wave Breaking in Deep Water', *J. Phys. Oceanog.* **16**, 382–385.

Taylor, P. K. and Yelland, M. J.: 2001, 'The Dependence of Sea Surface Roughness on the Height and Steepness of the Waves', *J. Phys. Oceanog.* **31**, 572–590.

Xu, D., Liu, X., and Yu, D.: 2000, 'Probability of Wave Breaking and Whitecap Coverage in a Fetch-Limited Sea', *J. Geophys. Res.* **105**, 14253–14259.

Yelland, M. and Taylor, P. K.: 1996, 'Wind Stress Measurements from the Open Ocean', *J. Phys. Oceanog.* **26**, 541–558.

Young, I. R. and Verhagen, L. A.: 1996, 'The Growth of Fetch Limited Waves in Water of Finite Depth. Part 2. Spectral Evolution', *Coastal Eng.* **29**, 79–99.